JOURNAL OF MAGNETIC RESONANCE, Series A 109, 157–165 (1994)

Theory and Exact Solutions for Tycko's Zero-Field NMR in High Field

B. Q. SUN AND A. PINES

Materials Sciences Division, Lawrence Berkeley Laboratory, 1 Cyclotron Road, Berkeley, California 94720; and Chemistry Department, University of California, Berkeley, California 94720

Received June 14, 1993; revised January 25, 1994

A theory of zero-field NMR in high field (ZFHF-NMR) is described in terms of coherent averaging and irreducible tensors. The theory is used to determine analytical solutions for the parameters of the trajectory proposed and used by Tycko. A new pulse sequence is presented, and optimized solutions for dynamic-angle spinning, dynamic-angle hopping, and double-rotation versions of ZFHF-NMR are discussed.

INTRODUCTION

High-resolution methods in solid-state NMR (*1–3*) are generally designed to reduce spectral broadening arising from anisotropic spin Hamiltonians, often by coherent averaging of either spatial or spin parameters. Such techniques, which include magic-angle spinning (MAS) (*4–6*), dynamic-angle spinning (DAS), and double rotation (DOR) (*7–10*), may be applied to polycrystalline materials, where ordinarily the signals originating from crystallites with different orientations would exhibit different resonance frequencies. These frequencies become time-dependent under certain externally imposed motions, and the signals observed thus can be made to reflect the isotropic averages of the original interaction tensors. An entirely different approach to eliminating anisotropy, however, is provided by time-domain zero-field NMR and NQR (*11, 12*), in which the sudden removal of the strong polarizing field renders the Hamiltonian isotropic by eliminating any preferred direction in space.

One class of time-domain zero-field methods relies on a field-cycling technique (*13, 14*) involving a series of steps: (1) polarization in high field, (2) adiabatic transport of the sample to an intermediate field of approximately 0.01 T, (3) a sudden quenching of the intermediate field to precipitate coherent evolution under an isotropic Hamiltonian, and (4) transport back to high field for detection. In this way the evolution of the system in zero field is mapped out indirectly, point by point, while the initial polarization and subsequent detection in high field preserve the advantage of high sensitivity. The zero-field spectrum so obtained consists of sharp spectral lines from whose frequencies the principal values of the spin interactions can be measured; there is, in principle, no broadening attributable to a dispersion of orientation-dependent resonance frequencies.

For such a method to be effective, however, the sample must have a sufficiently long relaxation time, T_1, so as to maintain the high-field polarization over the course of the experiment. Another drawback is the difficulty of achieving selective excitation of a particular nuclear species, inasmuch as all Larmor frequencies are equal to zero in zero field. To overcome these problems, one might ask whether it is possible to directly obtain the equivalent of zero-field spectra in high field, without ever resorting to field cycling. Indeed, in a beautiful series of studies (*15–18*), Tycko has shown that this goal can be realized by exploiting the fact that, in a coupled spatial–spin coordinate system, the high-field spin Hamiltonian can be represented by a linear combination of irreducible tensors from rank zero to four. Among these is the zero-rank tensor, which carries both isotropic and anisotropic information about the spin interactions and transforms as a scalar operator. This zero-rank tensor is exactly equivalent to the zero-field spin Hamiltonian and consequently may yield high-resolution spectra. Thus the strategy behind observing zero-field spectra in high field involves averaging out the high-rank tensors and leaving only the scalar part of the total Hamiltonian.

In this paper, we review the theory of zero-field NMR in high field as originally described by Tycko, using coherent averaging methods, and then obtain analytical solutions for the parameters used in Tycko's pulse sequence. These solutions are useful for achieving high-quality spectra. A new pulse sequence is presented, and optimized solutions for various sample spinning and hopping (*18, 19*) experiments are discussed.

BRIEF REVIEW OF ZERO-FIELD NMR IN HIGH FIELD

As a reminder, we follow the arguments of Tycko. A zero-field dipolar or quadrupolar spin Hamiltonian can be represented by an inner product of two second-rank tensors: one reflecting the spatial behavior and the other reflecting the spin behavior (*20*). Expressed in terms of irreducible tensors, the spin Hamiltonian is

1064-1858/94 $6.00

$$\mathcal{H} = \sum_{m=-2}^{2} (-1)^m A_{2,-m} T_{2,m}, \qquad [1]$$

where $T_{2,m}$ and $A_{2,m}$ are components of a second-rank spin and spatial tensor, respectively. Although Eq. [1] involves orientation-dependent terms, the whole expression for the Hamiltonian is, of course, invariant under a full rotation operation on the spatial and spin operators. However, after application of a strong external magnetic field along a particular direction (the z axis) in the laboratory frame, the rotational symmetry of the spin Hamiltonian is reduced from $SO(3)$ to C_∞. In other words, the Zeeman interaction is usually so large that the internal spin Hamiltonian is effectively truncated. To explicitly represent the truncated Hamiltonian, we first transform the spin Hamiltonian from the laboratory frame to the rotating frame (equivalently, the interactive picture) by the unitary operator $\exp(-i\mathcal{H}_z t)$, where $\mathcal{H}_z$ is the Zeeman Hamiltonian. The spin Hamiltonian in the rotating frame is then time-dependent. According to coherent averaging theory, the zero-order average Hamiltonian contains only the time-independent term of the total spin Hamiltonian and thus becomes

$$\mathcal{H} = A_{2,0} T_{2,0}. \qquad [2]$$

We can reconstruct a scalar Hamiltonian from Eq. [2] by representing the spin Hamiltonian in terms of a single set of irreducible tensors, $\{\mathcal{T}_{l,m}\}$, which are the product tensors of $A_{2,m}$ and $T_{2,m}$. This is equivalent to transforming the spin Hamiltonian from separate spatial and spin systems into a single, coupled spatial–spin system. The combined space is the direct product of the spatial and spin terms, and the $\{\mathcal{T}_{l,m}\}$ transform as tensors in this space. Using the multiplication properties of two irreducible tensors (*21, 22*), we write the product of the $A_{2,m}$ and $T_{2,m}$ as

$$A_{l_1,m_1} T_{l_2,m_2} = \sum_{l=|l_1-l_2|}^{l_1+l_2} C(l_1, l_2, m_1, m_2) \mathcal{T}_{l,m_1+m_2}, \qquad [3]$$

with $C(l_1, l_2, m_1, m_2)$ being the Clebsch–Gordan coefficients. Inserting Eq. [3] into Eq. [2] yields

$$\mathcal{H} = \sum_{l=0,2,4} C(2, 2, l, 0, 0) \mathcal{T}_{l,0}, \qquad [4]$$

in which no odd-rank tensors appear owing to the symmetry properties of the spin interaction. The zero-order tensor $\mathcal{T}_{0,0}$ is proportional to the scalar Hamiltonian given in Eq. [1], with a proportionality coefficient of $1/\sqrt{5}$ (which can be calculated from Eq. [4]). In combination with the Clebsch–Gordan coefficient of $\mathcal{T}_{0,0}$, $1/\sqrt{5}$, the coefficient of the scalar component in Eq. [4] therefore becomes $1/5$, causing a corresponding fivefold reduction in the resonance frequencies from those in time-domain zero-field NMR.

The remaining terms in Eq. [4], being orientation-dependent, cause anisotropic broadening in a powder sample. It would therefore be desirable to remove these terms from the Hamiltonian by applying motional-averaging techniques familiar from high-resolution solid-state NMR, in order to obtain what amounts to zero-field NMR spectra in high field. However, conventional high-resolution NMR techniques cannot be directly applied without some modifications, such as synchronization of the sample rotation with an applied pulse sequence. In the following paragraphs, we discuss specifically how such zero-field NMR in high field can be produced.

A rotation operator in the coupled spatial–spin system is written as

$$\mathcal{R}(\Omega) = R(\Omega_R) P(\Omega_P), \qquad [5]$$

where $R(\Omega_R)$ represents a sample rotation and $P(\Omega_P)$ is a spin rotation arising from RF pulses. All rotation operators in Eq. [5] are defined by Euler angles: α denotes the spin angle, β the nutation angle, and γ the precession angle. Application of a rotation operator $\mathcal{R}(\Omega)$ to the spin Hamiltonian (*4*) yields

$$\mathcal{H} = \sum_{l=0,2,4} \sum_{m=-l}^{l} C(2, 2, l, 0, 0) \mathcal{D}^{(l)}_{m,0}(\Omega) \mathcal{T}_{l,m}, \qquad [6]$$

where $\mathcal{D}^{(l)}_{m,0}(\Omega)$ are the components of Wigner rotation matrices. Since one of the two indices of the Wigner rotation matrix components in Eq. [6] is zero, it is possible to discard γ from the three Euler angles involved in the averaging. The Wigner rotation matrices in Eq. [6] still allow two degrees of freedom for manipulation of the spin Hamiltonian, however, via the rotation angle α and the rotation axis angle β. Furthermore, we are free to apply more than one rotation in the coupled spatial–spin system to obtain a zero-order average spin Hamiltonian given by

$$\bar{\mathcal{H}} = \frac{1}{N} \sum_{k=1}^{N} \sum_{l=0,2,4} \sum_{m=-l}^{l} C(, 2, 2, l, 0, 0) \mathcal{D}^{(l)}_{m,0}(\Omega_k) \mathcal{T}_{l,m}$$
$$= \sigma \mathcal{T}_{0,0}, \qquad [7]$$

where σ is a scaling factor (its maximum value being $\frac{1}{5}$ if $\mathcal{T}_{0,0}$ is normalized), and Ω_k are the Euler angles of the kth rotation. Any choice of N and Ω_k which satisfies Eq. [7] will be a valid trajectory for achieving zero-field NMR in high field. In order to find the optimum trajectories, however, it is desirable to have a general procedure analogous to that used for averaging of second-order quadrupole interactions (*9*).

Assume that a number of rotations, N_α, is applied along a fixed axis inclined at the angle β_k with respect to the z axis

in the coupled spatial–spin space. Averaging over the N_α rotations results in truncation of the spin-Hamiltonian Eq. [6] to

$$\bar{\mathcal{H}}(\beta_k) = \frac{1}{N_\alpha} \sum_{l=0,2,4} C(,2,2,l,0,0) d^{(l)}_{0,0}(\beta_k) \mathcal{T}_{l,0}, \quad [8]$$

in which the $d^{(l)}_{0,0}(\beta_k)$ are the elements of the reduced Wigner rotation matrices.

If the applied rotations are discrete (that is, with finite angle at well-defined times), the sequence must satisfy the condition

$$\sum_{k'=1}^{l+1} \exp(-im\alpha_{k'}) = \begin{cases} l+1 & \text{if } m = 0 \\ 0 & \text{if } m \neq 0, \end{cases} \quad [9]$$

with rotation angles of

$$\alpha_{k'} = \frac{2\pi k'}{l+1}, \quad [10]$$

and with the total number of rotations given as $N_\alpha = l + 1$, where l is the highest rank of the irreducible tensors in the spin Hamiltonian. In our case, $l = 4$ and $N_\alpha = 5$, which requires that the rotations involved in the truncation of Eq. [6] possess at least fivefold symmetry.

If the applied rotations are continuous, arising, say, from sample spinning at a rate ω_r, then the average over one rotation cycle is

$$\int_0^{2\pi/\omega_r} \exp(-im\omega_r t)dt = \begin{cases} 2\pi/\omega_r & \text{if } m = 0 \\ 0 & \text{if } m \neq 0, \end{cases} \quad [11]$$

where $N_\alpha = 2\pi/\omega_r$ is the normalization factor.

We next choose a suitable set of rotation axes, $\{\beta_k\}$, from which will follow, after the averaging, the scalar Hamiltonian given in Eq. [7]. If the rotations are discrete, the set of the rotation axis angles, $\{\beta_k\}$, must satisfy

$$\frac{1}{N_\alpha N_\beta} \sum_k C(2,2,l,0,0) d^{(l)}_{0,0}(\beta_k) = \begin{cases} \sigma & \text{if } l = 0 \\ 0 & \text{if } l \neq 0, \end{cases} \quad [12]$$

where N_β is the number of rotation axes. Alternatively, if the time dependence of the rotation axes is made continuous by rotating the sample about two or more axes simultaneously, the condition to obtain a scalar Hamiltonian becomes

$$\frac{1}{N_\alpha} C(2,2,l,0,0) \prod_k d^{(l)}_{0,0}(\beta_k) = \begin{cases} \sigma & \text{if } l = 0 \\ 0 & \text{if } l \neq 0, \end{cases} \quad [13]$$

with $N_\beta = 1$. Equations [9]–[13] thus present four general conditions for establishing trajectories capable of affording zero-field NMR spectra in high field.

EXACT SOLUTIONS OF TYCKO'S PULSE SEQUENCE

The first trajectory for obtaining zero-field NMR spectra in high field was proposed by Tycko (*15, 16*). In his original experiment, the sample rotates around an axis inclined at the angle $\beta_r = 75°$ with respect to the external field, while the pulse sequence shown in Fig. 1 is applied. The pulse sequence, displaying fivefold symmetry, consists of five blocks and is synchronized with the sample spinning. Each block has a phase increment of 72° and contains two pairs of delta RF pulses. Each pair with two pulses applies a discrete rotation (along a transverse axis in the rotating frame) to the spin operators. The phases of the two spin rotation axes in the kth block are $\varphi_{2k} = 2k\varphi + \phi_1$ and $\varphi_{2k+1} = 2k\varphi + \phi_2$, where $\varphi = \omega_r\tau = 36°$; 2τ is the duration of each block, $\phi_1 = 0°$ and $\phi_2 = 158°$ are the initial phases of the two rotation axes of the first block, and the nutation angles of all spin rotations are $\beta_1 = \beta_2 = \beta_p = 46°$. This pulse sequence produced a high-resolution zero-field NMR spectrum of a 95% deuterated solid benzene sample in high field. The spectrum, for a pair of protons, consists of three spectral lines with splitting equal to the dipole–dipole coupling constant multiplied by a scaling factor of 0.089. More solutions for various spin systems are also given by Tycko in Ref. (*17, 18*).

Here we express Tycko's pulse sequence within the framework of the general tensor formalism. We assume that the

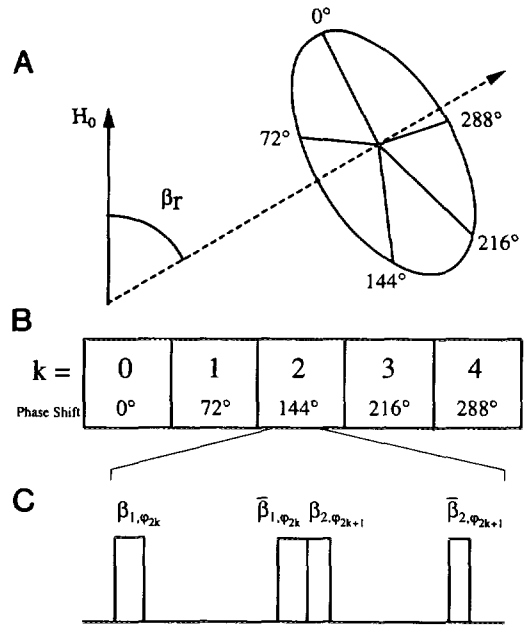

FIG. 1. Generalization of Tycko's trajectory. (A) The rotor cycle. The sample rotates at an angle β_r with respect to the external field, at an angular velocity $\omega_r = 2\pi/10\tau$. (B) The synchronized pulse sequence. Each block is phase shifted by 72° from the previous one. (C) Details of one pulse-sequence block; β_1, β_2 are the flipping angles, with phases $\varphi_{2k} = 2k\varphi + \phi_1$, $\varphi_{2k+1} = 2k\varphi + \phi_2$, and $\varphi = \omega_r\tau = 36°$.

sample rotates around a fixed axis oriented at an arbitrary angle with respect to the external magnetic field and consider what kind of pulse sequence is needed to make the zero-order average Hamiltonian a scalar.

According to group theory (*23*), five orientations equally distributed over a period of 2π can average to zero tensors up to fourth rank—with the exception of the zero-rank tensor, which is a scalar. The realization of fivefold symmetry in this case is accomplished by applying five rotational operations to the spin Hamiltonian in the coupled spatial–spin system. Each rotation has an increment of 72° in the spin angle α relative to the previous one, and the average over the fivefold symmetic operation removes any α dependence from the Hamiltonian. Practically, this can be implemented in such a way that one rotational cycle is divided into five equal arcs separated by 72° increments. Within each arc, the pulse sequence shown in Fig. 1c is applied to the spin operators of the Hamiltonian. This sequence consists of four pulses and involves two discrete spin–rotation operators with fixed rotation-axis angles (the nutation angles, β). According to average Hamiltonian theory (*1, 2*), we are not concerned with the exact trajectory of the Hamiltonian during one spinning period. What is important, however, are the initial and final values of the spatial tensors over this time, and these two values are obviously dependent on both the spinning speed and the initial position of the sample. As was described in the last section, in order to form a scalar Hamiltonian, the spin tensors should have the same values as those of the spatial tensors at the beginning and at the end of a period. This is the reason why two discrete rotation operators for the spin operators in the Hamiltonian are needed: one is used to control the initial phase, and the other determines the final phase of the spin tensors in each rotation cycle.

The propagator associated with the pulse sequence applied during the kth rotation of a period is

$$\begin{aligned}\mathcal{L}_k(\tau) = &\exp(-i\beta_2 I_{\varphi_{2k+1}})\exp[-i\bar{\mathcal{H}}_{2k+1}(\tau)]\\ &\times \exp(i\beta_2 I_{\varphi_{2k+1}})\exp(-i\beta_1 I_{\varphi_{2k}})\\ &\times \exp[-i\bar{\mathcal{H}}_{2k}(\tau)]\exp(i\beta_1 I_{\varphi_{2k}}),\end{aligned} \quad [14]$$

where

$$\begin{aligned}\varphi_{2k} &= 2k\varphi + \phi_1\\ \varphi_{2k+1} &= 2k\varphi + \phi_2\\ \varphi &= \omega_r\tau = 36°,\end{aligned} \quad [15]$$

and where the phases ϕ_1 and ϕ_2 are constant for each pulse. The zero-order average Hamiltonian, $\bar{\mathcal{H}}_k(\tau)$, over the sample spinning in the time interval τ is

$$\bar{\mathcal{H}}_k(\tau) = \sum_m B_m(\tau)\exp(-ikm\omega_r\tau)A_{2,m}T_{2,0}, \quad [16]$$

for which

$$B_m(\tau) = \begin{cases}(i/m\omega_r)[\exp(-im\omega_r\tau) - 1]d^{(2)}_{m,0}(\beta_r) & \text{for } m \neq 0\\ d^{(2)}_{0,0}(\beta_r)\tau & \text{for } m = 0,\end{cases} \quad [17]$$

and β_r is the angle of the rotation axis with respect to the external field.

By the end of a cycle, the total propagator under zero-order approximation is

$$\mathcal{L}(\tau_c) = \prod_{k=0}^{4}\mathcal{L}_k(\tau) = \exp(-i\bar{\mathcal{H}}\tau_c). \quad [18]$$

Since

$$\sum_{k=0}^{4}\exp[-ik(m + m')\varphi] = \begin{cases}0 & \text{if } m + m' \neq 0\\ 5 & \text{if } m + m' = 0,\end{cases} \quad [19]$$

Eqs. [14]–[17] allow us to write the total zero-order average Hamiltonian, $\bar{\mathcal{H}}$, as

$$\begin{aligned}\bar{\mathcal{H}} = &\frac{1}{\tau_c}\sum_{m,m'}B_m\left[\sum_{k=0}^{4}\exp[-ik(m + m')\varphi]\right]\\ &\times [\exp(-im'\phi_1)d^{(2)}_{m',0}(\beta_1)\\ &+ \exp[-i(m\omega_r\tau + m'\phi_2)]d^{(2)}_{m',0}(\beta_2)]A_{2,m}T_{2,m'}\\ = &\frac{5}{\tau_c}\sum_m B_{-m}[\exp(-im\phi_1)d^{(2)}_{m,0}(\beta_1)\\ &+ \exp[-im(\phi_2 - \omega_r\tau)]d^{(2)}_{m,0}(\beta_2)]A_{2,-m}T_{2,m}.\end{aligned} \quad [20]$$

From Eq. [20], the zero-order average Hamiltonian becomes a scalar operator only if

$$\begin{aligned}&\frac{5}{\tau_c}B_{-m}[\exp(-im\phi_1)d^{(2)}_{m,0}(\beta_1)\\ &\quad + \exp[-im(\phi_2 - \omega_r\tau)]d^{(2)}_{m,0}(\beta_2)] = (-1)^m\sigma,\\ &\qquad m = -2, \ldots, 2,\end{aligned} \quad [21]$$

where σ is a scaling factor. In Eq. [21], there are six unknowns (β_r, β_1, β_2, ϕ_1, ϕ_2, σ) and five complex simultaneous equations for different m. Due to the symmetry of Wigner rotation matrices, only three equations are independent, which can be written as five real simultaneous equations (for $m = 0$, the equation is already real). Only five unknowns can be

determined by these equations, and therefore one out of the six unknowns is as a free variable. By redefining the phase variables as

$$\phi_1' = \phi_1 - \tfrac{1}{2}\varphi$$
$$\phi_2' = \phi_2 - \tfrac{3}{2}\varphi, \qquad [22]$$

where $\varphi = \omega_r\tau = 36°$, it is possible to express the five real equations as

$$\frac{1}{2} d^{(2)}_{0,0}(\beta_r)[d^{(2)}_{0,0}(\beta_1) + d^{(2)}_{0,0}(\beta_2)] = \sigma$$
$$-\frac{5}{\pi}\sin\left(\frac{1}{2}\varphi\right) d^{(2)}_{-1,0}(\beta_r)[d^{(2)}_{1,0}(\beta_1)\cos(\phi_1') + d^{(2)}_{1,0}(\beta_2)\cos(\phi_2')] = \sigma$$
$$\frac{5}{2\pi}\sin(\varphi) d^{(2)}_{-2,0}(\beta_r)[d^{(2)}_{2,0}(\beta_1)\cos(2\phi_1') + d^{(2)}_{2,0}(\beta_2)\cos(2\phi_2')] = \sigma$$
$$d^{(2)}_{1,0}(\beta_1)\sin(\phi_1') + d^{(2)}_{1,0}(\beta_2)\sin(\phi_2') = 0$$
$$d^{(2)}_{2,0}(\beta_1)\sin(2\phi_1') + d^{(2)}_{2,0}(\beta_2)\sin(2\phi_2') = 0. \qquad [23]$$

Equation [23] can be easily solved in the case of $\beta_1 = \beta_2 = \beta_p$, with the solution determined by a quadratic equation

$$x^2 + Bx + C = 0, \qquad [24]$$

in which

$$x = \tan^2(\beta_r)$$
$$B = \frac{1}{2}\left[\frac{15}{2\pi}\sin(\varphi)\cos(2\phi_1') - 1\right]C - 2$$
$$C = \frac{16\cos^2(\phi_1')}{\cos^2(\frac{1}{2}\varphi)\cos^2(2\phi_1')} \qquad [25]$$

and where ϕ_1' is a free parameter that can take any value between 0 and 2π. After obtaining β_r from Eqs. [24] and [25], we can calculate the other two variables, β_p and ϕ_2', as

$$\tan(\beta_r)\tan(\beta_p) = \pm\sqrt{C}$$
$$\phi_2' = -\phi_1'. \qquad [26]$$

Moreover, from Eq. [25], it follows that the coefficients B and C have a period of π with respect to the ϕ_1'; that is, the values of B and C at ϕ_1' are the same as those at $\phi_1' + \pi$.

Figure 2 shows β_r, β_p, and σ as functions of ϕ_1'. From the figure it can be clearly seen that solutions of β_r, β_p, and σ exist only in the region of $\phi_1' \in (32.69°, 147.31°)$. In principle, solutions of β_r and β_p are interchangeable, but for practical convenience we define the angle of the sample rotation axis, β_r, to be in the range of 0° to 90°. The pulse angle β_p has two sets of solutions varying from −71° to 71°, and each set exhibits an inverse symmetry about $\beta_p = 0°$ and $\phi' = 90°$. The solutions of β_r and σ are symmetric around $\phi' = 90°$.

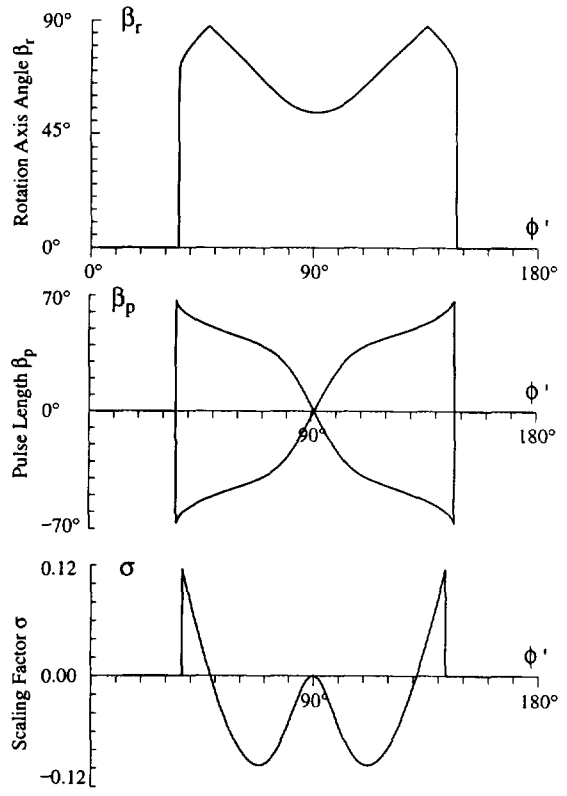

FIG. 2. Exact solutions of β_r, β_p ($\beta_1 = \beta_2 = \beta_p$) and σ as functions of the free variable ϕ_1' in period [0°, 180°]. The zero-order average Hamiltonian is a scalar operator attenuated by a factor of σ relative to the untruncated internal spin Hamiltonian for each set of ϕ_1', β_r, and β_p.

The largest absolute value of the scaling factor σ is located at $\phi_1' = -\phi_2' = 32.689°$ or $\phi_1 = 50.689°$ and $\phi_2 = 21.311°$, with $\beta_r = \beta_p = 71.064°$. At this point, $\sigma = 0.117$. A more stable solution at which the first-order derivative of the scaling factor to the free variable is zero is found at $\beta_r = 69.505°$, $\beta_p = 42.864°$ and $\phi_1 = 84.375°$, $\phi_2 = -12.375°$, where $\sigma = -0.0966$. Another stable solution corresponds to the magic angle, at which $\sigma = 0$.

In Fig. 3a, static powder patterns are presented for asymmetry parameters of $\eta = 0$ and $\eta = 0.5$. Figure 3b shows the corresponding high-resolution spectra containing the same information. Experimentally, zero-field NMR spectra in high field can be achieved only when the spinning speed ω_r is large compared with the internal spin interactions (dipolar

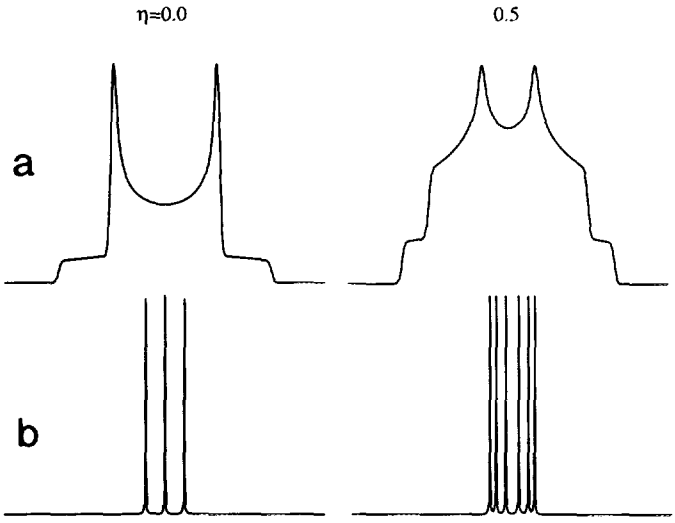

FIG. 3. Computer-simulated (a) powder patterns for $\eta = 0$ and $\eta = 0.5$ and (b) "zero-field" spectra obtained by applying rotation synchronized with the pulse sequence ($\phi_1 = 84.375$, $\beta_r = 69.505$, $\beta_p = 42.864$, and $\sigma = -0.0966$), for $\eta = 0$ and $\eta = 0.5$.

or quadrupolar coupling). This will be the major obstacle for applying the method to extract the principal values of the quadrupolar interactions. However, the experiments performed by Tycko (*18*) have shown the potential applications of the method for studying coupled lone-pair proton systems in which the dipolar couplings have been scaled down by random internal motions.

AN ALTERNATIVE SEQUENCE FOR ZERO-FIELD NMR IN HIGH FIELD

In Tycko's trajectory, a mechanical sample rotation is synchronized with discrete pulses to obtain an effective scalar Hamiltonian. In this section, we describe an alternative trajectory, also based on average Hamiltonian theory, in which both the spatial and the spin parts of the Hamiltonian are modulated by continuous rotations, but the orientation of the axis of one of the rotations is allowed to suddenly change, as is the phase of the spinning. In practice this feature can be conveniently applied to the spin rotation, since it is more difficult to mechanically change the spatial sample rotation axis. Another characteristic of the new trajectory is that the total average Hamiltonian is obtained over two rotation cycles, which may affect the efficiency of the sample spinning with respect to a single spin interaction. If chemical-shift anisotropy (CSA) is present, Tycko's trajectory also requires two cycles in order to accommodate a refocusing π pulse.

We start with the rotating-frame spin Hamiltonian given by Eq. [2]. Application of spatial and spin rotations to this Hamiltonian yields

$$\begin{aligned}\mathcal{H}(t) &= \sum_{m_1,m_2} \mathcal{D}^{(2)}_{m_1,0}(\Omega_r)\mathcal{D}^{(2)}_{m_2,0}(\Omega_p)A_{2,m_1}T_{2,m_2} \\ &= \sum_{m_1,m_2} \exp[-i(m_1\omega_r + m_2\omega_p)t] \\ &\quad \times \exp[-i(m_1\varphi_r + m_2\varphi_p)] \\ &\quad \times d^{(2)}_{m_1,0}(\beta_r)d^{(2)}_{m_2,0}(\beta_p)A_{2,m_1}T_{2,m_2}, \qquad [27]\end{aligned}$$

where ω_r and ω_p are the spinning speeds of the spatial and spin rotations, respectively, φ_r and φ_p are the initial phases of the rotations, and β_r and β_p are the angles of the rotation axes with respect to the external field. In order to produce a scalar Hamiltonian, the indices of the spatial and spin tensors must satisfy the relationship given in Eq. [1]: $m_2 = -m_1 = m$. The spinning speeds of the two rotations therefore must be equal ($\omega_r = \omega_p = \omega_b$), and the resulting zero-order average Hamiltonian is given by

$$\begin{aligned}\bar{\mathcal{H}} &= \sum_m \exp[-im(\varphi_p - \varphi_r)] \\ &\quad \times d^{(2)}_{-m,0}(\beta_r)d^{(2)}_{m,0}(\beta_p)A_{2,-m}T_{2,m}. \qquad [28]\end{aligned}$$

It can be shown that for a single pair of rotations around fixed axes it is impossible to obtain the zero-field scalar Hamiltonian given by Eq. [1]. The next step is to consider whether two pairs of rotations can extract the scalar operator from the total spin Hamiltonian in high field. As in the preceding section, we choose to keep the angle of the spatial rotation axis with respect to the external field constant and change instead the phase and axis of the spin rotation. After application of average Hamiltonian theory over two rotation cycles, the problem is reduced to finding the solution of the equation

$$\begin{aligned}&\tfrac{1}{2}d^{(2)}_{-m,0}(\beta_r)[\exp(-im\varphi_{p_1})d^{(2)}_{m,0}(\beta_{p_1}) \\ &\quad + \exp(-im\varphi_{p_2})d^{(2)}_{m,0}(\beta_{p_2})] = (-1)^m\sigma, \qquad [29]\end{aligned}$$

in which we have already set $\varphi_r = 0$.

Looking for the simplest solutions of Eq. [29], we set $\varphi_{p_1} = \varphi_{p_2} = 0$. Equation [29] then reduces to the set of three simultaneous equations

$$\begin{aligned}&\tfrac{1}{2}d^{(2)}_{0,0}(\beta_r)[d^{(2)}_{0,0}(\beta_{p_1}) + d^{(2)}_{0,0}(\beta_{p_2})] = \sigma \\ &\tfrac{1}{2}d^{(2)}_{-1,0}(\beta_r)[d^{(2)}_{1,0}(\beta_{p_1}) + d^{(2)}_{1,0}(\beta_{p_2})] = -\sigma \\ &\tfrac{1}{2}d^{(2)}_{-2,0}(\beta_r)[d^{(2)}_{2,0}(\beta_{p_1}) + d^{(2)}_{2,0}(\beta_{p_2})] = \sigma. \qquad [30]\end{aligned}$$

Equation [30] not only looks simpler than Eq. [23], but there are also only four unknown variables, one of which is independent.

The dependence of the solutions of Eq. [30] (β_r, β_{p_1}, σ) on the free variable β_{p_2} is shown in Fig. 4. Because of the

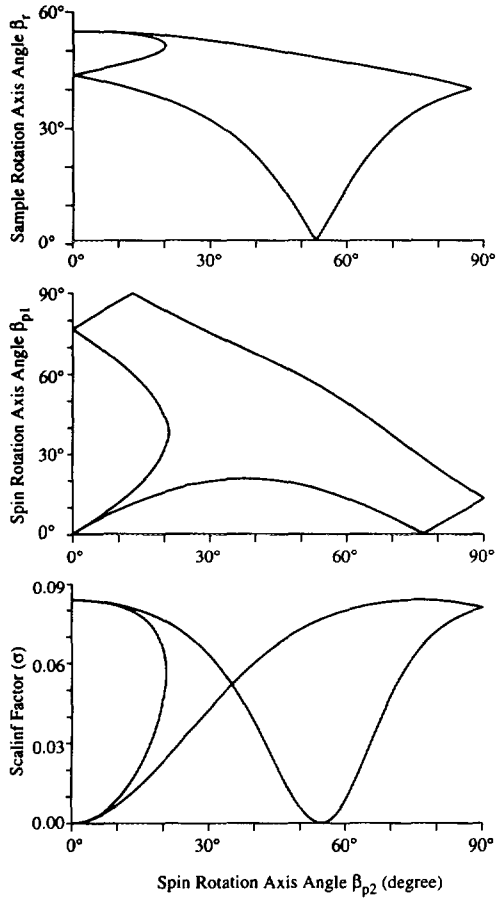

FIG. 4. Exact solutions of β_r, β_{p_2}, and σ as functions of the free variable β_{p_1} in the [0°, 180°] period. The zero-order average Hamiltonian is a scalar operator scaled by a factor σ from the untruncated internal spin Hamiltonian for each set of β_{p_1}, β_{p_2}, and β_r.

symmetry properties of Eq. [30], if β_i ($i = p_1, p_2, r$), is one of the solutions of Eq. [30], so is $\pi - \beta_i$. For this reason, we show angles of the solutions only in the region of 0° to 90°. As can be seen from the figure, for each value of β_{p_2}, there two sets of β_r, β_{p_1}, and σ values for each solution in the region of [20.603°, 90°] and four sets in the region of [0°, 20.603°]. For magic-angle spinning of the sample, or when both β_{p_1} and β_{p_2} are magic angles, the scaling factor is zero.

The maximum scaling factor that can be obtained from this trajectory is 0.084 (corresponding to $\beta_r = 43.48°$, $\beta_{p_1} = 76.66°$, and $\beta_{p_2} = 0°$), smaller than the value 0.117 in Tycko's trajectory. Nevertheless, this trajectory is derived from a simple pulse sequence and is stable at the point with maximum scaling factor. The most interesting solution of this trajectory is at $\beta_{p_2} = 0°$ with maximum scaling factor. At this point we need not apply any RF field in the first period because the rotation around the z axis in the rotating frame commutes with the spin Hamiltonian, and thus the spin parts of the Hamiltonian are unaffected during the rotation. As in the case of Tycko's trajectory, the mechanical rotation must be synchronized with the RF fields, the amplitude as well as the phase. Experimentally, the axes and rates of the spin rotation may be adjusted by changing the offset and the amplitude of the RF field (*24*), as in the rotating-frame magic-angle experiment of Lee and Goldburg (*25*).

OPTIMIZED SOLUTIONS

Three solutions are readily obtained from Eqs. [12] and [13]. These solutions coincide with the trajectories used in dynamic-angle spinning and double rotation (*7, 8*) and in dynamic-angle hopping (DAH) (*9*), which are used to eliminate the second-order line broadenings of the central transitions in half-integer quadrupolar nuclei. The similarity arises because the second-order line broadenings are determined by both the second- and the fourth-rank spatial tensors of the first-order average Hamiltonian in the rotating frame. The theory behind these trajectories is also similar (*10, 18*), the main difference being that all the rotations applied in the zero field in the high-field experiment are performed in the coupled spatial–spin system. We briefly show here some of the results.

The first set of trajectories can be obtained by directly solving Eqs. [9] and [12] using discrete rotations. These solutions consist of a series of "hops" of the z axis in the coupled spatial–spin space along paths given by two cones. On each cone, the solutions consist of five points separated by equal increments of 72°. Ten hops are therefore needed. Experimentally, these sudden changes can be implemented by moving the quantization axes of the spin interaction in the coupled spatial–spin space simultaneously. Although the hops in spin space can be made quickly by applying RF pulses, it is much more difficult to move the sample mechanically. Practically, sample hopping can be implemented by storing the magnetization along the external magnetic field (where the magnetization relaxes very slowly), changing the orientation of the sample in the laboratory frame, and finally bringing back the magnetization to the xy plane for further evolution. Alternatively, the same result may be achieved (while retaining both components of the magnetization) by using synchronized π pulses (*26*). The solution that minimizes the number of hops is a path defined by the vertices of an icosahedron (Fig. 5).

In this experiment, which we term dynamic-angle hopping in analogy to magic-angle spinning (*19*), the half-apex angle θ is zero for the first cone and 63.43° for the second cone. In a DAH cycle, the sample and the magnetization hop through six vertices on the icosahedron, with the magnetization evolving for a time $\tau/6$ (where τ is the length of a cycle) under the spin Hamiltonian given by Eq. [6]. When the sample and the magnetization have traced a closed path through all six vertices of the icosahedron, the average Ham-

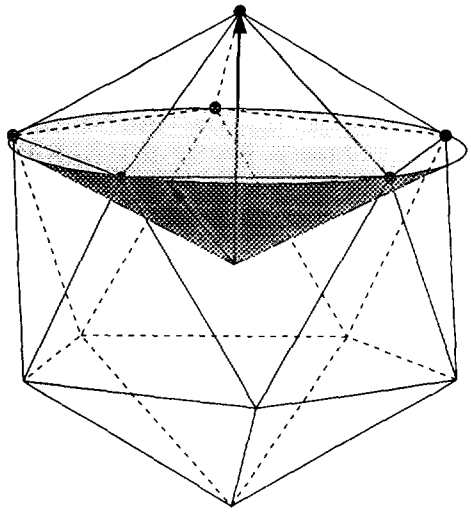

FIG. 5. Dynamic-angle-hopping (DAH) trajectory: an icosahedron. The half-apex angle of the first cone (indicated by the vertical arrow) is $\theta^{(1)} = 0°$ and the half-apex angle of the second cone (shaded region) is $\theta^{(2)} = 63.43°$ with respect to the external field.

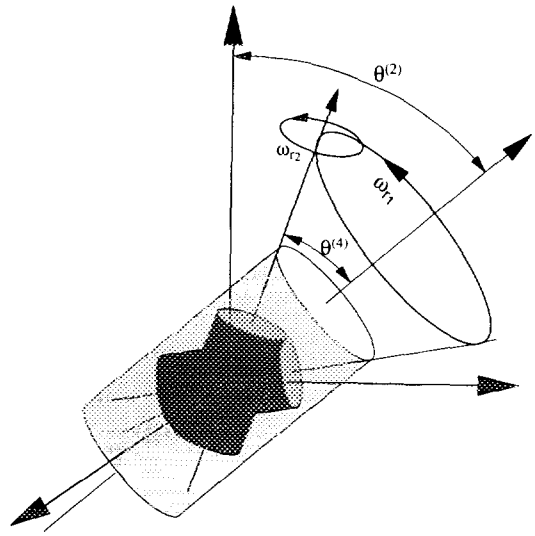

FIG. 7. Double-rotation (DOR) trajectory. The first rotation axis is tilted at $\theta^{(2)} = 54.74°$, the magic angle of the second-order Legendre polynomial, with respect to the external field. The second rotation axis is at $\theta^{(4)} = 30.56°$, one of the magic angles of the fourth-order Legendre polynomial, relative to the first rotation axis.

iltonian is a scalar in which the coupling constants δ_λ of quadrupolar or dipolar interactions are reduced by a factor of five ($\sigma = \frac{1}{5}$).

Instead of using discrete rotations (or hops), the z axis of the coupled spatial–spin system may also travel continuously on the two concentric cones. On the first cone, the spins evolve for a time t_1, while on the second cone, they evolve for a time t_2 under the Hamiltonian in Eq. [6]. The half-apex angles of the two cones depend on the ratio of the two evolution times t_1/t_2. If the ratio is 1, the first half-apex angle is given by $\beta_1 = \theta^{(1)} = 37.38°$ and the second half-apex angle by $\beta_2 = \theta^{(2)} = 79.19°$. This trajectory possesses a dodecahedral symmetry (see Fig. 6). Five vertices of the dodecahedron are located on the cone with half-apex angle $\theta^{(1)}$, while the other five vertices of the polyhedron are located on the cone with half-apex angle $\theta^{(1)}$, while the other five vertices of the polyhedron are located on the cone with half-apex angle $\theta^{(2)}$. This trajectory corresponds to DAS (7) for zero-field NMR in high field, and, as in DAH, it yields coupling constants reduced by a factor of five ($\sigma = \frac{1}{5}$).

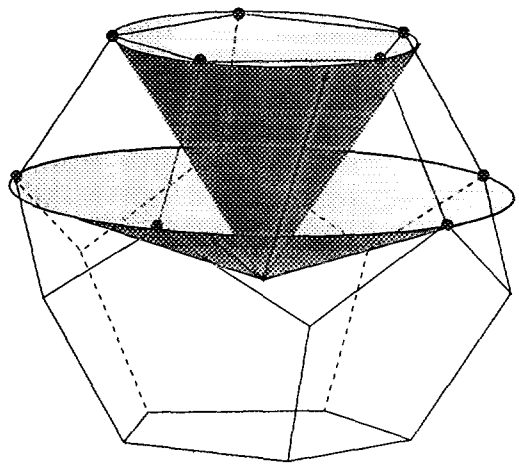

FIG. 6. Dynamic-angle-spinning (DAS) trajectory: a dodecahedron. The half-apex angle of the first cone (top shaded portion) is $\theta^{(1)} = 37.38°$ and the half-apex angle of the second cone (bottom shaded portion) is $\theta^{(2)} = 79.19°$ with respect to the external field.

In the previous two trajectories, the discrete or continuous rotations applied to the z axis of the coupled spatial–spin space occur at different times. According to Eq. [13], a zero-field spin Hamiltonian can also be achieved by rotating the z axis of the coupled spatial–spin space around two or more axes simultaneously A scalar Hamiltonian results when one of the axes is tilted at $\beta_1 = \theta^{(2)} = 54.74°$ (the "magic" angle of the second-order Legendre polynomial) with respect to the static magnetic field H_0 and the second axis of the rotations is at $\beta_2 = \theta^{(4)} = 30.56°$ (one of the magic angles of the fourth-order Legendre polynomial) relative to the first axis (see Fig. 7). This trajectory corresponds to DOR (8) for zero-field NMR in high field. The scaling factor of the coupling constants with DOR trajectory is again $\sigma = \frac{1}{5}$.

CONCLUSIONS

In summary, we have provided an analytical basis for solutions to Tycko's ZFHF-NMR experiment, and we have shown one alternative pulse sequence and a number of optimized solutions for maximal scaling factors.

ACKNOWLEDGMENTS

This work was supported by the Director, Office of Energy Research, Office of Basic Energy Sciences, Materials Sciences Division, of the U.S. Department of Energy under Contract DE-AC03-76SF0098. We are grateful to Erwin Hahn, Antoine Llor, and Robert Tycko for helpful comments.

REFERENCES

1. U. Haeberlen, "Principles of High Resolution NMR in Solids," 2nd ed., Springer-Verlag, Berlin/New York, 1983.
2. M. Mehring, "High Resolution NMR in Solids," 2nd ed., Springer-Verlag, Berlin/New York, 1983.
3. C. P. Slichter, "Principles of Magnetic Resonance," 3rd ed., Springer-Verlag, Berlin/New York, 1989.
4. E. R. Andrew, A. Bradbury, and R. G. Eades, *Nature* **182,** 1659 (1958).
5. I. J. Lowe, *Phys. Rev. Lett.* **2,** 285 (1959).
6. M. M. Maricq and J. S. Waugh, *J. Chem. Phys.* **70,** 3300 (1979).
7. K. T. Mueller, B.-Q. Sun, G. C. Chingas, J. W. Zwanziger, T. Terao, and A. Pines, *J. Magn. Reson.* **86,** 470 (1990).
8. A. Samoson, E. Lippmaa, and A. Pines, *Mol. Phys.* **65,** 1013 (1988); A. Lior and J. Virlet, *Chem. Phys. Lett.* **152,** 248 (1988).
9. A. Samoson, B. Q. Sun, and A. Pines, *in* "Pulsed Magnetic Resonance: NMR, ESR and Optics—A Recognition of E. L. Hahn" (D. M. S. Bagguley, Ed.), Clarendon Press, Oxford, 1992.
10. B. Q. Sun, J. H. Baltisberger, Y. Wu, A. Samoson, and A. Pines, *Solid State NMR* **1,** 267 (1992).
11. D. P. Weitekamp, A. Bielecki, D. Zax, K. Zilm, and A. Pines, *Phys. Rev. Lett.* **50,** 1807 (1983).
12. A. M. Thayer and A. Pines, *Acc. Chem. Res.* **20**(2), 47 (1987).
13. R. V. Pound, *Phys. Rev.* **81,** 278 (1951).
14. D. T. Edmonds, *Phys. Rep.* **29,** 233 (1977).
15. R. Tycko, *J. Magn. Reson.* **75,** 193 (1987).
16. R. Tycko, *Phys. Rev. Lett.* **60,** 2734 (1988).
17. R. Tycko, G. Dabbagh, J. C. Duchamp, and K. W. Zilm, *J. Magn. Reson.* **89,** 205 (1990).
18. R. Tycko, *J. Chem. Phys.* **92,** 5778 (1990).
19. N. M. Szeverenyi, A. Bax, and G. E. Maciel, *J. Magn. Reson.* **61,** 440 (1985).
20. A. Abragam, "Principles of Nuclear Magnetism," Clarendon Press, Oxford, 1982.
21. M. E. Rose, "Elementary Theory of Angular Momentum," Wiley, New York, 1957.
22. B. L. Silver, "Irreducible Tensor Methods," Academic Press, New York, 1962.
23. M. Hamermesh, "Group Theory and Its Application to Physical Problems," Addison-Wesley, Reading, Massachusetts, 1962.
24. A. E. Mefed, *Sov. J. Exp. Theoret. Phys.* **86,** 302 (1984).
25. M. Lee and W. I. Goldburg, *Phys. Rev. A* **140,** 1261 (1965).
26. S. L. Gann, J. H. Baltisberger, and A. Pines, *Chem. Phys. Lett.* **210,** 405 (1993).